

# Coastal Erosion Dynamics in Nakhon Si Thammarat Province, Thailand: A Decadal Analysis (1990–2025)

Yuhang, H. and Wutjanam, M.\*

Department of Civil and Environmental Engineering, Faculty of Engineering, Mahidol University, Thailand

E-mail: huyuhang2023@163.com, wutjanam.mut@mahidol.ac.th\*

\*Corresponding Author

DOI: <https://doi.org/10.52939/ijg.v21i9.4451>

## Abstract

*This study develops and applies a reproducible remote-sensing workflow to analyze coastal erosion and accretion dynamics in Nakhon Si Thammarat Province, Thailand, over the period 1990–2025. Leveraging Landsat 5, 8, and 9 archives on the Google Earth Engine (GEE) platform, the method integrates the Automated Water Extraction Index (AWEI) with Otsu thresholding in a semi-automated pipeline for consistent coastline detection across sandy, muddy, and mangrove-dominated coasts. This approach minimizes subjectivity in threshold selection, harmonizes data across sensors, and allows large-scale, long-term monitoring with reproducibility. Results reveal severe erosion in Pak Phanang Bay and Hua Sai (–3 to –5 m/yr, with localized extremes exceeding –30 m/yr), moderate retreat along southern muddy coasts, and notable accretion at Laem Talumphuk (+32.63 m/yr) and river mouths due to sediment deposition. The workflow not only highlights the drivers of change—monsoon storms, sea-level rise, aquaculture expansion, and coastal engineering—but also demonstrates the capacity of GEE-based methods to provide actionable, repeatable insights for coastal management. This methodological innovation offers a scalable template for monitoring vulnerable coastlines globally, supporting the design of adaptive, evidence-based strategies in the face of accelerating sea-level rise and intensifying climate impacts.*

**Keywords:** AWEI, Coastal Erosion, DSAS, Google Earth Engine, Otsu Thresholding, Shoreline Change

## 1. Introduction

Coastal erosion is a global phenomenon threatening approximately 70% of the world's sandy coastlines [1]. In Thailand, it is a severe environmental challenge, with over 600 kilometers of coastline considered critically eroding [2]. Coastal zones of the Gulf of Thailand are subject to a wide range of physical and anthropogenic stresses from seasonal monsoon storms and long-term sea-level rise to coastline engineering and land-use change that together drive complex patterns of erosion and accretion [3]. The coastal plain of Nakhon Si Thammarat (NST) combines mangrove-fringed estuaries, sandy beaches, and urbanised coastlines, and has been identified repeatedly as a region of high vulnerability [4]. Baseline assessments and local monitoring have reported segments of critically eroding coastline, with historical observations of very large local retreat, in some places exceeding 5 m/yr [5].

Over the last three decades, freely available satellite archives (chiefly the Landsat series) and cloud-computing platforms such as Google Earth Engine (GEE) have transformed how coastline

change is quantified at regional to national scales [6]. Several studies have demonstrated the value of these tools: GEE workflows have been used successfully for multi-decadal mangrove mapping and wall-to-wall change detection [7][8][9] and [10], while automated toolkits and time-series extraction methods, such as CoastSat paired with DSAS, have been applied to digitise coastline positions and derive rates of change across hundreds of kilometres of coastline [11] and [12]. These remote-sensing approaches make it possible to track coastline dynamics across both sandy beaches and mangrove systems, and to produce reproducible mosaics and long-term time series. Application of these methods to southern Thailand has already revealed highly variable behaviour at the provincial scale. For example, a recent coastline-digitisation effort across Krabi and Nakhon Si Thammarat (1990–2019) reported extreme local variability, ranging from rapid mangrove progradation to severe mangrove loss and substantial erosion on sandy coasts, highlighting both hotspots of retreat and areas of stability [12].

At the same time, broader assessments that combine remote sensing with sea-level and socio-economic data have emphasised that local erosion trends are driven by a mix of natural forcing and human interventions such as coastal defense structures, reclamation, and land-use change [13].

Despite these advances, important gaps remain. Many coastlines change studies for NST stop around 2019, leaving the most recent half-decade, a period marked by severe monsoon events, continued sea-level rise, and new infrastructure projects largely undocumented. Moreover, while existing approaches have demonstrated the feasibility of automated coastline extraction, few have developed a fully reproducible GEE-based pipeline that harmonises Landsat data across sensors and accounts for different coastline types, including mangroves, sandy coasts, and engineered structures. In response to these gaps, the present study aims to extend the Landsat-derived coastline record for Nakhon Si Thammarat through to 2025 using a GEE-based workflow. The objectives are threefold: first, to generate a consistent, multi-decadal time series (1990–2025) of coastline positions by harmonising Landsat data and applying robust cloud and atmospheric corrections; second, to quantify spatial and temporal patterns of erosion and accretion across different coastline types, thereby identifying critical hotspots of change; and third, to examine these patterns in relation to potential drivers, including sea-level rise and coastal engineering interventions, so as to provide evidence that can support management and adaptation strategies.

By combining the full Landsat archive with the processing capacity of GEE, this study seeks to provide timely and reproducible insights into the dynamics of one of Thailand's most vulnerable coastal provinces.

## 2. Methodology

### 2.1 Study Area

Nakhon Si Thammarat Province is an area that has experienced historical sea retreat over the past 6,000 years [14], during the Holocene period. Evidence suggests the presence of several former sandy beaches interspersed with peat swamps formed by seawater accumulation. Nakhon Si Thammarat is located on the eastern coast of the Malay Peninsula in Southern Thailand, along the Gulf of Thailand. The province's coordinates are approximately 7°50'N to 9°20'N, and 99°10'E to 100°20'E. The province's coastline stretches approximately 236.82 kilometers [12], covering six districts and 25 sub-districts: Khanom, Sichon, Tha Sala, Mueang, Pak Phanang, and Hua Sai. It begins at the coast of Khanom District

and continues southward through Sichon District. This coastline features rocky shores and barrier beaches. Farther south, the coastline runs parallel to the mainland in Tha Sala and Mueang Nakhon Si Thammarat Districts, continuing to Pak Phanang Bay, where the intertidal flats give way to mangrove forests.

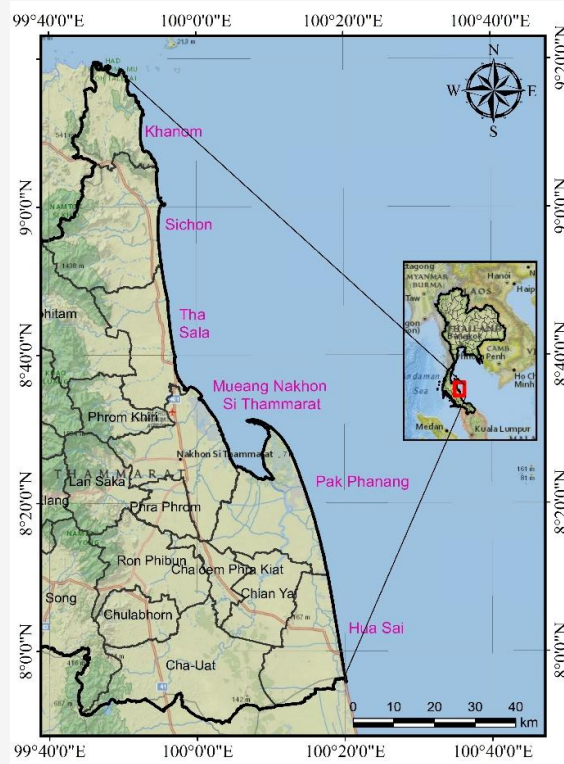


**Figure 1:** Nakhon SI Thammarat coastline

The coastline is characterized by north-south-oriented sandy beaches, beginning at the tip of the sandbar at Laem Talumphuk and continuing to the beaches of Ranot District in Songkhla Province (Figure 1). The coastline of Nakhon Si Thammarat is considered one of the most vulnerable areas to coastal change in Thailand. Coastal erosion is a significant issue here, driven by a combination of natural processes and human activities. The province experiences high rates of erosion, with some areas seeing a coastline retreat of over 5 m/yr [4]. Certain studies have even documented much higher rates of up to 33 meters per year in specific sections [15]. This erosion is intensified by extreme weather events like monsoons and tropical storms, which are frequent in the region from September to January and cause heavy rainfall, flash floods, and coastal inundation [16].

Human factors such as the development of aquaculture farms, particularly shrimp farming [17], and coastal infrastructure like breakwaters and jetties have also been identified as contributing to or exacerbating the problem by disrupting natural sediment flow [18]. As a result, the province's coastal communities and infrastructure are facing significant threats from land loss and flooding

## 2.2 Data Used

The data for this study consists of time-series imagery from the Landsat program, specifically from Landsat 5, 8, and 9 satellites, spanning the period from 1990 to 2025. This long-term dataset is crucial for monitoring and analyzing coastal changes over a multi-decadal period. The images were processed using the Google Earth Engine (GEE) platform, a cloud-based geospatial analysis tool that provides access to the entire Landsat archive and a powerful processing environment [19]. The use of GEE is particularly advantageous for this type of research due to its ability to handle large volumes of data without the need for significant local storage and computing power [20].

All available cloud-free images from the Landsat satellites within the specified time frame were utilized. Cloud masking, a critical step in pre-processing satellite data for coastal studies, was performed within GEE to ensure that the analysis was based on clear-sky observations. The raw images, which contain digital numbers representing at-sensor radiance, were converted to a more suitable format, such as surface reflectance, to account for atmospheric effects and allow for consistent comparisons over time. The coastlines were extracted automatically using algorithms available in the Google Earth Engine environment. These methods typically involve leveraging the distinct spectral properties of water and land, often by calculating water index as the Automated Water Extraction Index (AWEI). The index uses specific bands from the Landsat imagery to enhance the contrast between water and non-water features. Once a binary land-water image is created, a vector coastline is extracted, which is then used for the change detection analysis. This automated process, performed at a planetary scale on the GEE platform,

## 2.3 Automated Water Extraction Index

The Automated Water Extraction Index (AWEI) is a spectral index designed to effectively delineate water bodies, particularly in complex landscapes where other indices, such as the Normalized Difference Water Index (NDWI), may fail [21]. AWEI's formulation is specifically optimized to suppress or eliminate confusion from non-water features that can

have similar spectral characteristics to water, such as mountain shadows, dark soil, or built-up areas. The AWEI algorithm is expressed by Equation 1 [22]:

$$AWEI = 4(Green - SWIR1) - 0.25NIR - 2.75SWIR2$$

Equation 1

Where *Green*, *SWIR1*, *NIR*, and *SWIR2* refer to the reflectance values of the corresponding spectral bands. The use of multiple bands, especially the shortwave-infrared (SWIR) bands, is critical to AWEI's effectiveness. Water strongly absorbs SWIR radiation, resulting in very low reflectance values, which AWEI leverages to create a strong contrast between water and non-water pixels. The output of the AWEI calculation is a grayscale image where water bodies are represented by high positive values and non-water features by lower or negative value [23].

## 2.4 Otsu Thresholding

Otsu's method is a global, non-parametric, and unsupervised technique for image binarization. It is widely used for automatically selecting an optimal threshold to partition an image's pixel histogram into two classes (e.g., foreground and background) [24]. The core principle of Otsu's method is to maximize the between-class variance, which is a measure of the separability of the two classes. The algorithm exhaustively searches for the threshold value ( $k$ ) that minimizes the intra-class variance or, equivalently, maximizes the inter-class variance, as defined by Equation 2[25]:

$$\sigma_b^2(k) = \omega_0(k)\sigma_0^2(k) + \omega_1(k)\sigma_1^2(k)$$

Equation 2

Where  $\omega_0$  and  $\omega_1$  are the probabilities of the two classes separated by the threshold, and  $\sigma_0$  and  $\sigma_1$  are their respective variances. By applying Otsu's method to the AWEI-derived image, the optimal threshold can be determined without manual intervention, which allows for consistent and reproducible water body extraction. This automated process is particularly valuable for large-scale or time-series analysis where manual threshold selection for each image would be impractical and prone to human error [26]. The combination of AWEI to enhance water features and Otsu's method for automated thresholding provides a robust and efficient methodology for accurate and reproducible water body extraction from satellite imagery, which is a critical component for many scientific studies involving hydrology, environmental monitoring, and climate research [27].

## 2.5 Coastline Extraction

The coastline detection was conducted using Google Earth Engine (GEE) with a semi-automated workflow integrating water index calculation, Otsu thresholding, edge detection, and vectorization. The method builds upon previous work on Canny edge detection and Otsu thresholding [28] and coastline extraction [29]. The coastline extraction process illustrated in Figure 2 can be summarized in the following steps:

### 1. Data Collection and Preprocessing

Landsat data (Collection 2, Tier 1 Level-2) was selected for the target study area (Nakon Si Thammarat province). The images were filtered based on the temporal window (January 1, to December 31 for 1990 – 2020, while January 1 to June 31 for 2025) and the area of interest. A cloud- and shadow-masking algorithm was applied using the QA\_PIXEL band. Bitwise operations removed pixels contaminated by clouds and shadows. Radiometric scaling was applied to the optical bands (blue, green, red, NIR, SWIR1, SWIR2) to convert raw values to surface reflectance. A median composite was generated across all valid images to reduce noise from residual cloud contamination and temporal variability [30].

### 2. Water Detection Using AWEI and Otsu Thresholding

Water features were extracted using the AWEI index. To separate land and water pixels, an Otsu thresholding method was applied, which determines an optimal cutoff value from the AWEI histogram. Pixels above the threshold were classified as water, and those below as land. This reduced subjectivity compared to using a manually defined threshold [31].

### 3. Post-processing to Remove Inland Water and Small Islands

The binary water mask was refined by eliminating small inland water bodies and coastal islands that fall

below user-defined thresholds (2,000 m for waterbody size and 1,000 m for island size). This was achieved using connected component analysis, which removes small pixel clusters that are not part of the main coastline [32]. The result was a clean land-water boundary raster.

### 4. Coastline Vectorization and Simplification

The raster land-water boundary was converted into vector polygons using the `reduceToVectors()` function. To improve cartographic usability, the vector coastline was simplified by applying a tolerance equal to the export resolution (30 m). Buffering operations ensured that only true boundary lines were extracted while avoiding rasterization artifacts. The final output was a polyline representation of the coastline.

5. *Export of Results: The methodology produced three primary outputs as follows:*

- Composite image (cloud-free Landsat median composite)
- Land-water boundary raster (binary classification of land vs. water)
- Vector coastline shapefile (simplified polyline of extracted coastline)

These were exported to Google Drive in GeoTIFF and Shapefile formats for further analysis and cartographic use.

## 3. Results and Discussion

### 3.1 Overview of Coastline Change (1990–2025)

Analysis of the Landsat-derived coastline positions from 1990 to 2025 reveals pronounced spatial variability along the 236 km coastline of Nakhon Si Thammarat Province. The AWEI and Otsu thresholding workflow successfully separated land and water boundaries across both sandy and mangrove-dominated coasts, generating consistent coastline vectors for change detection.

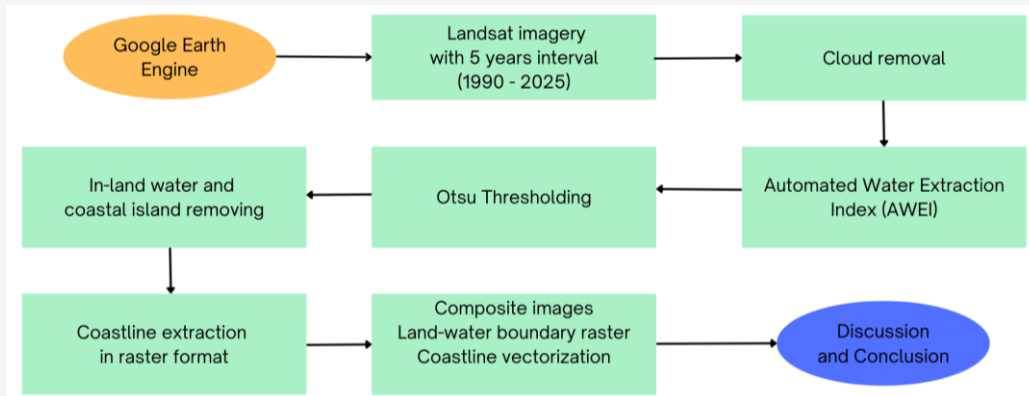


**Figure 2:** Coastline extraction

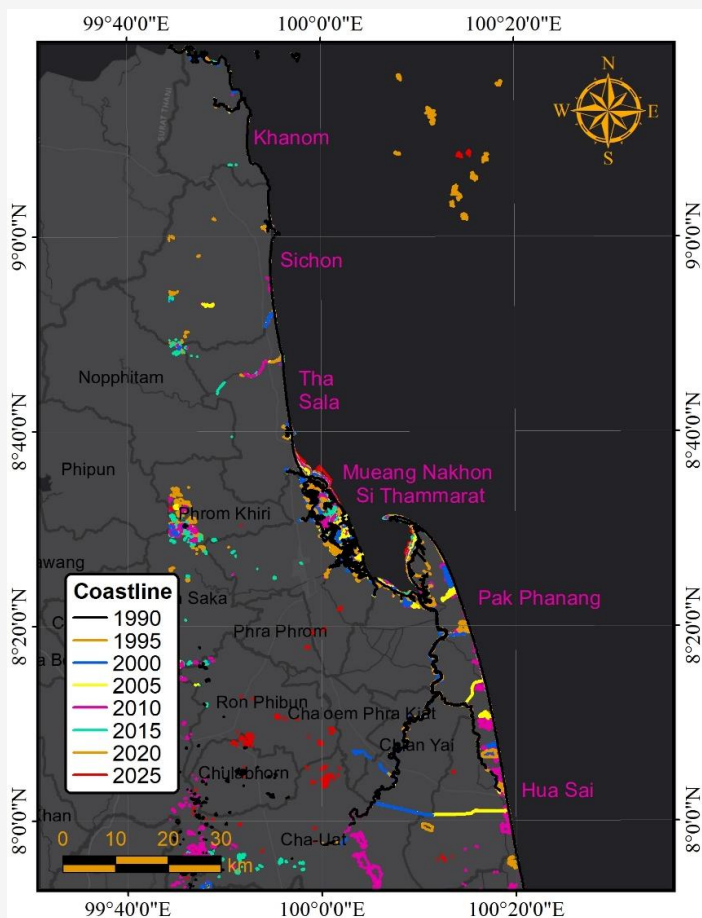


**Figure 3:** Coastal erosion from 1990 to 2025

The results in figure 3 demonstrate that while some sectors of the coastline have remained relatively stable or even accreted, other stretches exhibit significant retreat, in some cases at rates exceeding 5 m/yr. These divergent outcomes reflect a complex interplay of natural processes, such as monsoon-driven wave energy and relative sea-level rise, and anthropogenic pressures including shrimp farming, coastal infrastructure, and mangrove clearance.

### 3.2 Highest Erosion Areas

The coastline at Ban Koh Tang in the Pak Phanang district emerged as the most severely eroded sector during the 1990-2025 period, as presented in Figure 4. Within this area, the coastline receded by 183.78 m between 1990 and 2025, resulting in an average erosion rate of -5.25 meters per year (Figure 4(a)). This is considered a highly severe erosion rate, with increased erosion observed especially after major monsoon seasons. An erosion distance of 125.83 meters between 1990 and 2025 (with an average erosion rate of -3.59 m/year) was observed in the

eastern part of Pak Phanang district, as presented in Figure 4(b). Historical reports of extreme retreat, in some cases up to -30 m/yr during storm years [33] and [34], align with our findings of persistent coastline loss. The bay's geomorphology, a shallow estuarine system fringed by mangroves makes it highly sensitive to both fluvial sediment supply changes and wave energy. Upstream damming and river regulation have further reduced sediment delivery, while mangrove deforestation for aquaculture has diminished natural buffering capacity. Hard-engineering interventions such as groynes and seawalls, designed to protect critical assets, have provided localized stability but exacerbated downdrift erosion, accelerating retreat in unprotected stretches.

Another erosion hotspot is located along the southern muddy coast near the eastern part of Pak Phanang, where land loss has been driven by aquaculture conversion and storm surges. More recent studies have also identified substantial erosion rates along the wider NST coastline.

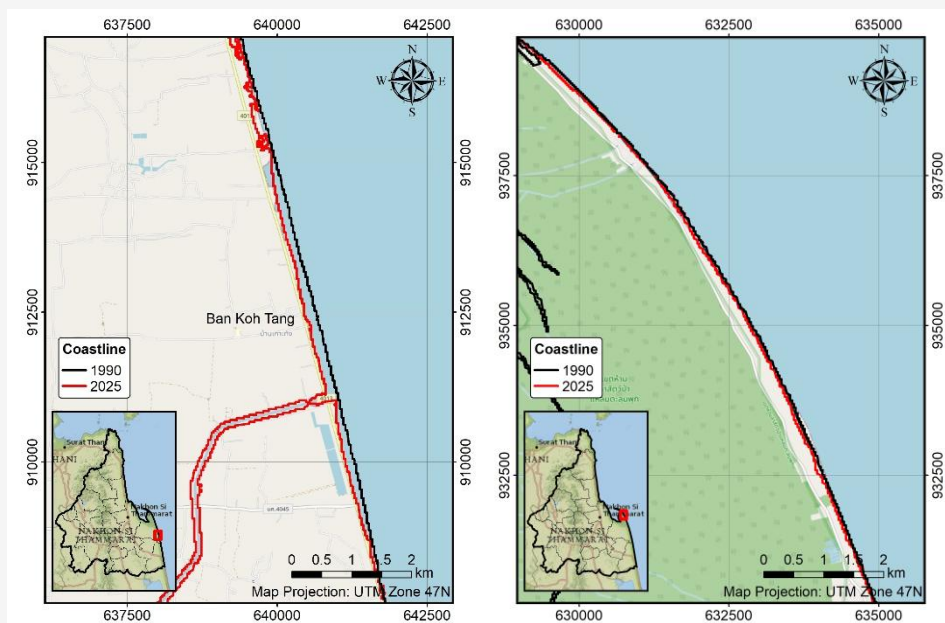


**Figure 4:** Erosion (a) severe erosion at Ban Koh Tang, Pak Phanang (b) moderate erosion at Pak Phanang

CoastSat toolkit and DSAS was used to investigate the NST erosion rate, the results found that the erosion rate varied dramatically, from a high of  $-66$  m/year in mangrove areas to  $-22.2$  m/year on sandy beaches. Another assessment noted that sections of the NST coast have experienced retreat rates of up to  $33.65$  m/year [12]. These figures underscore the severity of the problem, with many areas losing land at rates far exceeding the national average.

The causes of these high erosion rates are multifaceted. Natural factors, such as strong monsoonal currents, tidal forces, and rising sea levels, play a significant role. The region is frequently impacted by extreme stormy weather and tropical cyclones, which enhance coastal flooding and erosion. However, human activities have been a major accelerant. Intensive shrimp farming, which often involves the clearing of mangrove forests, has been identified as a contributing factor. The destruction of these natural barriers removes a crucial defense against wave energy, making the coast more susceptible to erosion. Furthermore, coastal protection structures, such as seawalls and rock revetments, while intended to solve erosion problems, can sometimes disrupt natural sediment transport and lead to accelerated erosion in adjacent areas.

### 3.3 Non-Erosion Areas

In contrast, several stretches of the NST coast have demonstrated relative stability as illustrates in Figure

5. Coastal erosion in the NST area has largely been characterized by stability from 1990 to 2025 as presents in Figure 5. This pattern is primarily attributed to the high volume of sediment supplied by the region's river systems and the protective function of expansive mangrove ecosystems. Rivers draining into the Gulf of Thailand carry substantial loads of terrestrial sediment, which are then deposited along the shoreline. This continuous supply of new material effectively counteracts any erosional forces, leading to a net gain of land over time. The high sediment budget is a fundamental reason why many coastal sections in Nakhon Si Thammarat are depositional rather than erosional. Furthermore, the widespread presence of mangrove forests acts as a critical natural defense against erosion. These ecosystems are highly effective at trapping and stabilizing sediment due to their intricate root systems. The dense network of aerial roots dissipates wave energy, reducing its erosive power, while the subsurface roots bind the soil, preventing its removal by currents and tides. In many areas, active reforestation efforts and natural mangrove regeneration have further strengthened this protective barrier. This biological resilience, combined with the ample sediment supply, has created a robust system that favors coastal stability and accretion, thereby explaining the predominance of non-coastal erosion zones in the Nakhon Si Thammarat region over the past three decades.

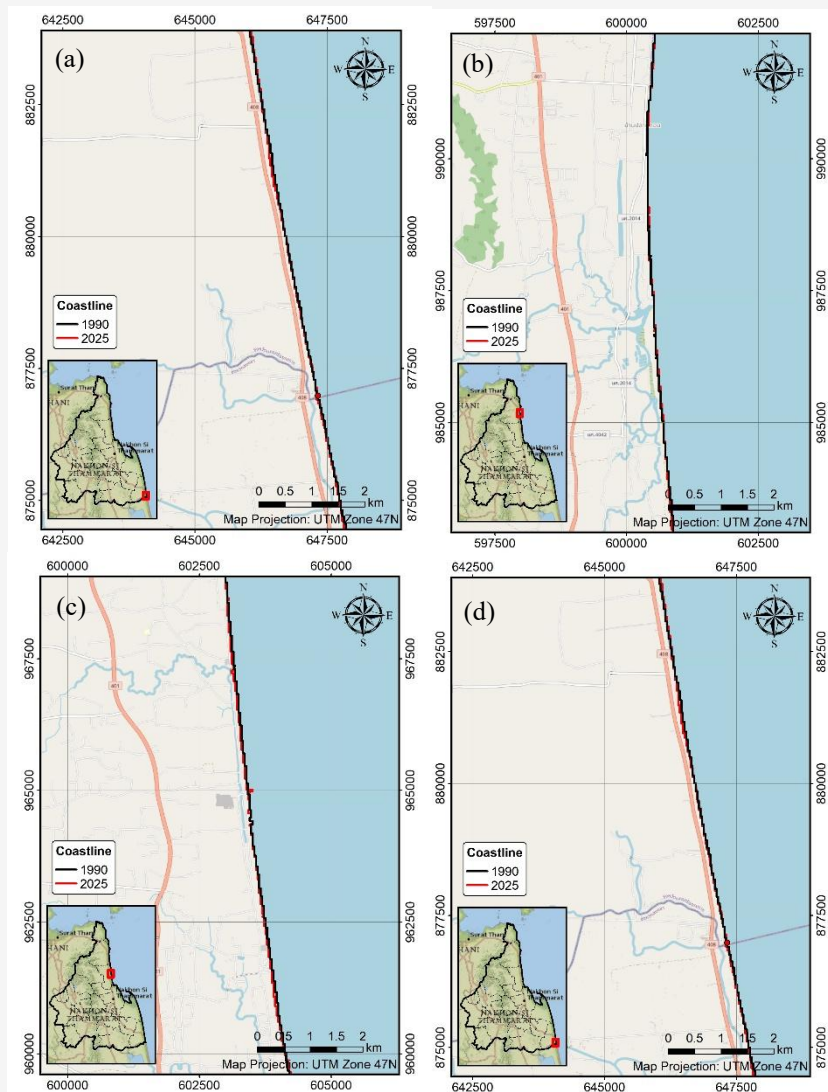


**Figure 5:** Non-erosion area (a) Khanom (b) Sichon (c) Tha Sala (d) Hua Sai

### 3.4 Accreting Areas

The coastline change in terms of accreting areas is illustrated in Figure 6 provide a clear spatial representation of the progradational processes active in the study area. Figure 6 reveals a clearly noticeable accreting area in the Pak Phanang district, particularly at Laem Talumphuk, a cape located in the northern part of the district. The accretion that occurred between 1990 and 2025 at the cape (Laem Talumphu) is presented in Figure 7.

It is evident that the accreting area increased by 1,142 meters since 1990, which corresponds to an average rate of approximately +32.63 m/year. Furthermore, Figure 8 also reveals significant accretion in the eastern parts of Pak Phanang and Mueang Nakhon Si Thammarat, which are located on the opposite side of Pak Phanang. Sediment accretion

and deposition rates have been consistently high at Laem Talumphuk and Mueang Nakhon Si Thammarat between 1990 and 2025 due to a combination of natural and anthropogenic factors. The primary natural drivers include the significant sediment load delivered by local rivers, which act as a major source of terrestrial material, particularly during seasonal monsoons. The region's exposure to monsoonal winds and tropical storm events further intensifies these processes, as high-energy waves and storm surges redistribute and deposit vast quantities of suspended sediment across the coastal zone. This dynamic interplay between fluvial input and coastal hydrodynamics creates an environment conducive to continuous and substantial sediment accumulation.

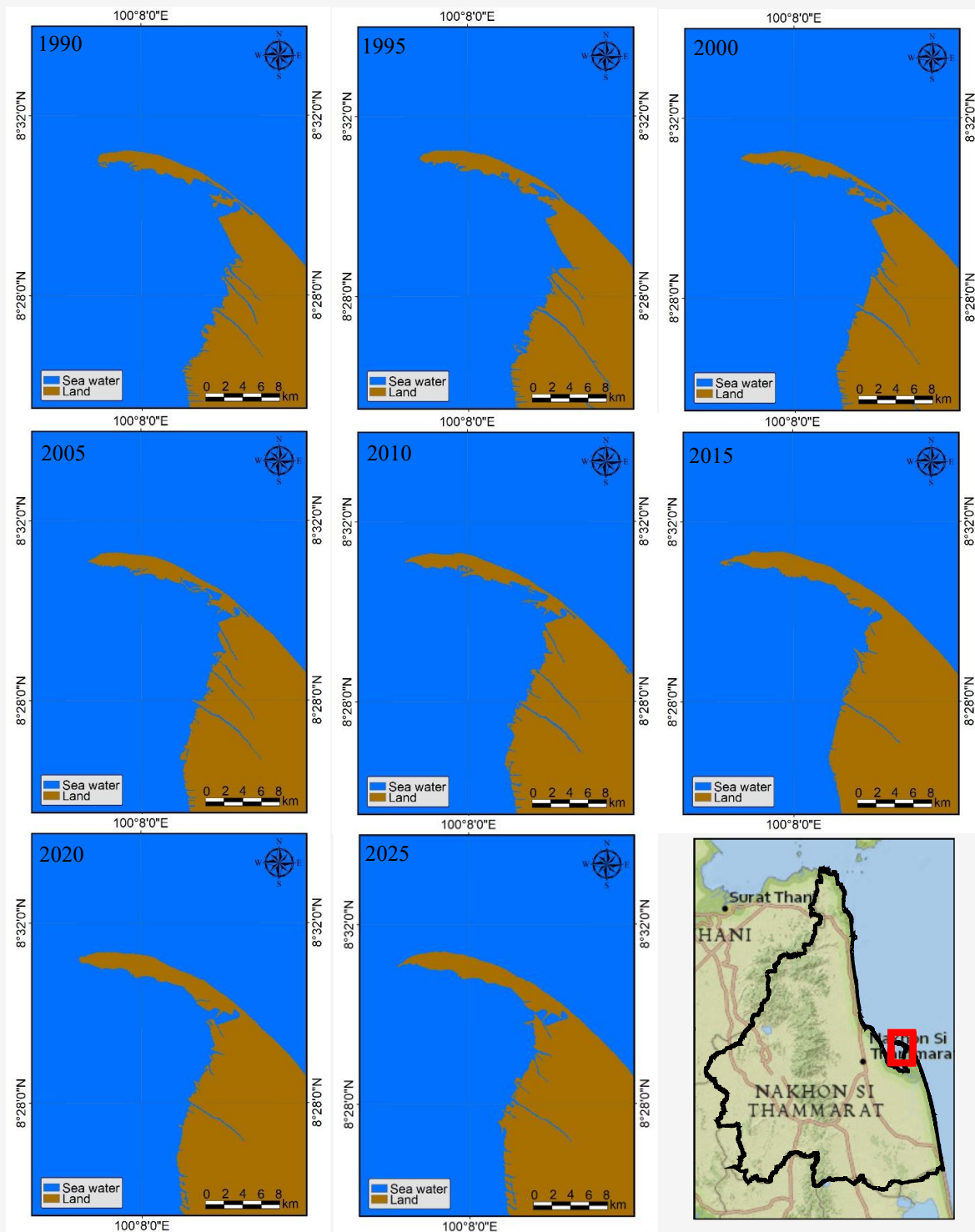


**Figure 6:** Coastal change at at Laem Talumphuk, Pak Phanang district, Nakhon Si Thammarat

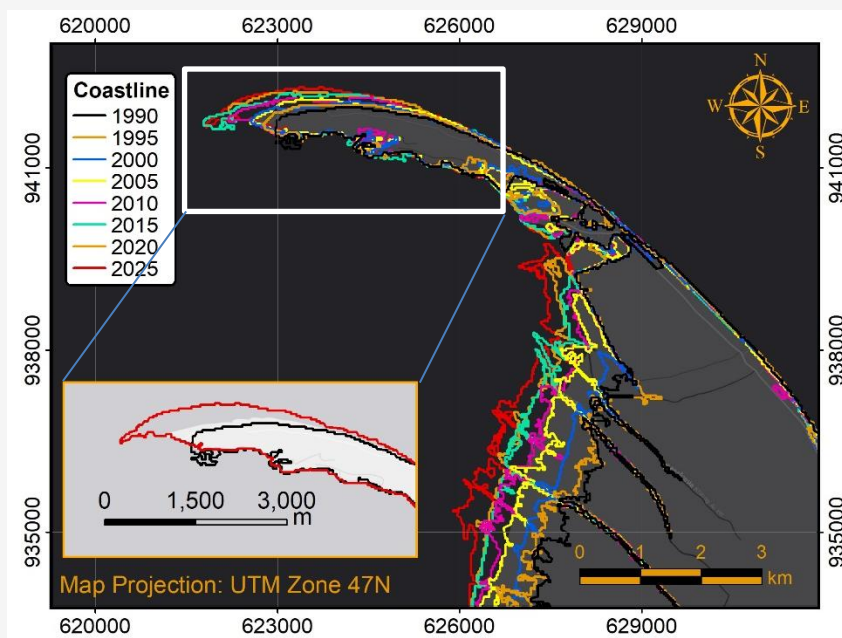


**Figure 7:** Accreting land in Laem Talumphuk from 1990 to 2025

In addition, some mangrove rehabilitation programs initiated in the early 2000s have enhanced sediment trapping and provided effective protection, leading to modest accretion in targeted restoration zones. Artificial accretion has also been recorded updrift of groynes and breakwaters, where sediment accumulation can reach +3 to +6 m/yr. However, these engineered accretion pockets are typically narrow and often paired with intensified erosion immediately downdrift, underscoring the trade-offs inherent in hard-structure interventions. The previous studies also noted positive shoreline changes, with accretion rates of up to +16.4 m/year in mangroves and +10.6 m/year on sandy beaches [12].

The primary reason for accretion in certain areas is the presence of natural coastal defenses, particularly mangrove forests. These ecosystems are vital for coastal protection, acting as natural barriers that absorb wave energy and stabilize sediment. Mangroves help to maintain a balance in the coastal ecosystem and can even help the coastline self-repair after damage from storms. The implementation of mangrove restoration projects has been shown to be effective in reducing erosion rates. In some cases, the construction of coastal protection structures, such as bamboo fences and rock revetments, has also contributed to a decline in erosion rates in specific locations [35] and [36].

Crucially, the presence of extensive mangrove ecosystems plays a pivotal role in mediating these depositional processes. The complex aerial root

systems of mangroves effectively reduce water flow, causing suspended particles to settle out of the water column. Once deposited, the dense root network below ground stabilizes the new sediment, preventing it from being re-eroded by tidal currents [37]. This biological feedback loop establishes a self-reinforcing system where sediment accretion facilitates mangrove growth, which in turn enhances further deposition and coastline stabilization. Coastal engineering structures, such as breakwaters, have also influenced localized sedimentation patterns by altering natural current and wave dynamics, leading to accelerated deposition in specific areas [38]. Significant changes in the agricultural area of Mueang Nakhon Si Thammarat district are presented in Figure 8. It is clearly observed that the agricultural area has increased since 1990, with seawater gradually transitioning into land. In 1990, some portions of the current agricultural land were still occupied by seawater, but over the following decades, this area expanded noticeably, replacing water surfaces with reclaimed land suitable for cultivation.

Despite these visible changes in land use, the coastline along this agricultural area has not shown evidence of significant erosion when applying the Otsu threshold method for coastline extraction. This suggests that the apparent expansion of agricultural land is not primarily due to retreat of the sea, but rather to land accretion and conversion processes inland.

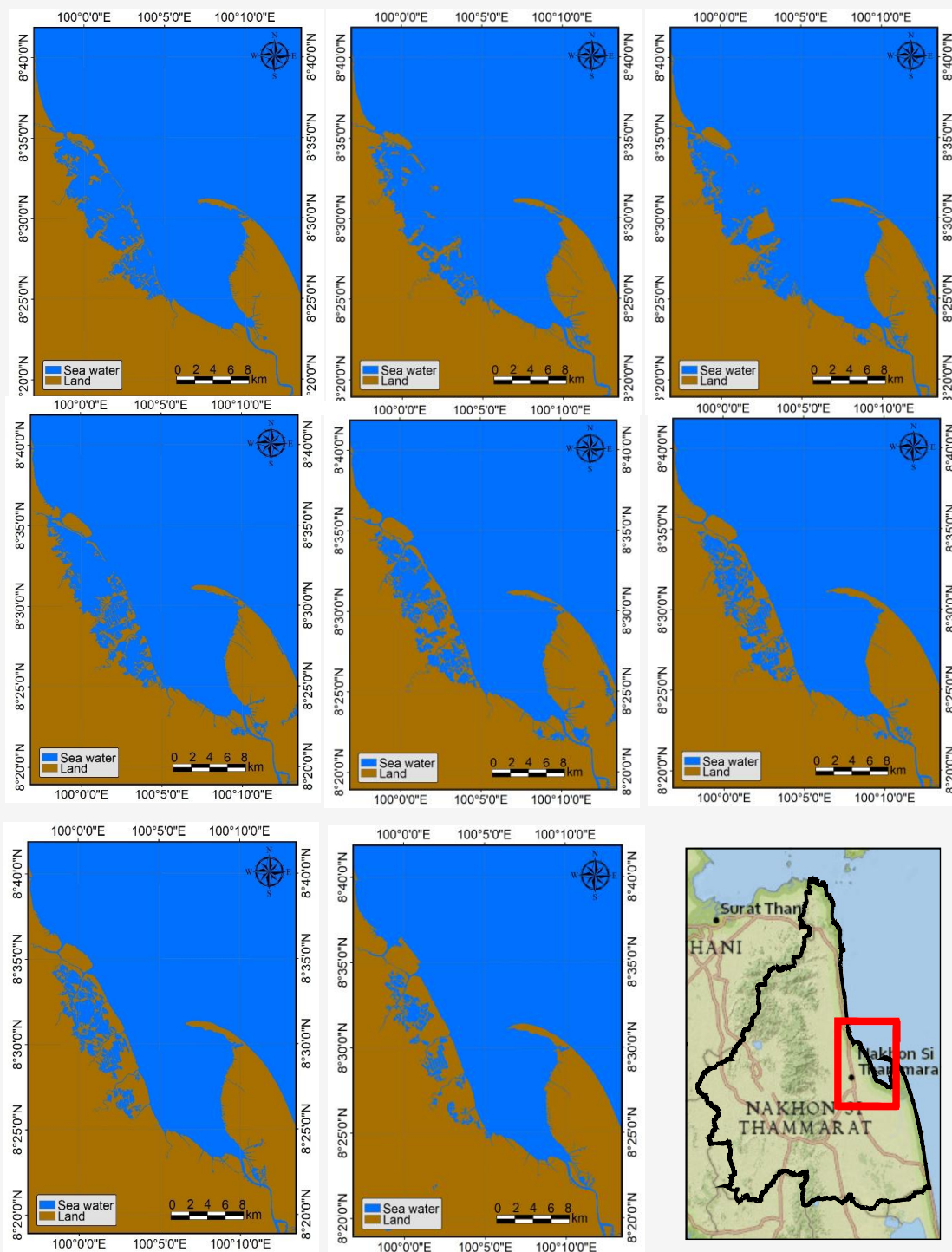


**Figure 8:** Coastal change at Mueang Nakhon Si Thammarat district

However, the binary images derived from the AWEI occasionally delineate a misleading boundary between land and water. This misclassification is particularly evident in agricultural zones where soil moisture, vegetation cover, or seasonal flooding can

confuse the spectral signature and cause water-like responses. Therefore, caution is needed when relying solely on AWEI for coastline mapping in complex environments where land-water transitions are influenced by both natural and anthropogenic factors.

To improve the reliability of coastline detection, the integration of composite images with the Otsu threshold algorithm is recommended. Composite imagery reduces seasonal and atmospheric noise by combining multiple images, while the Otsu method enhances the separation between land and water pixels. When applied together, these approaches can provide more consistent and accurate coastline extraction results compared to using AWEI alone

### 3.5 Coastline Change

Table 1 presents representative coastline change rates along the coast of NST between 1990 and 2025. The table serves to summarize the spatial diversity of coastline dynamics observed across different coastal settings in the province. By combining transect-based analyses with qualitative interpretation, it highlights areas of severe and persistent erosion, relatively stable or moderately retreating sectors, and localized accretion zones influenced by either natural processes or human interventions. The results illustrate that NST's coastline does not follow a uniform pattern but instead reflects a mosaic of geomorphological, hydrodynamic, and anthropogenic influences.

The most striking feature is the severe erosion in Pak Phanang Bay and its downdrift coastline, where retreat rates are typically between -3 and -5 m/yr, with certain hotspots exceeding this range. This sector has long been recognized as one of the most vulnerable stretches in Thailand, where multi-decadal land losses have been driven by reduced sediment supply, subsidence, and the compounded impacts of hard-structure interventions. The southern

muddy and mangrove-dominated coasts, outside Pak Phanang, also exhibit moderate to high erosion (-2 to -4 m/yr). Mangrove degradation and conversion to aquaculture have removed natural coastline stabilizers [39], while storm-driven erosion has further accelerated retreat. In these sectors, the loss of mangrove buffers has left low-lying areas exposed to flooding and land loss during seasonal monsoon surges.

In contrast, the northern sandy beaches of NST show much lower rates of retreat, averaging between 0 and -2 m/yr. Some sections remain relatively stable, benefiting from localized sediment inputs and less direct exposure to wave energy compared with the southern coasts. These areas highlight how geomorphology and wave climate influence the degree of coastline change. River mouth zones represent notable exceptions to the overall erosion trend, showing localized accretion at rates of +2 to +5 m/yr. Here, fluvial sediment deposition leads to the development of prograding spits and bars, although such positive trends are spatially limited and often offset by erosion in adjacent sectors. The influence of coastal engineering is also evident in the table. On the updrift side of groynes and breakwaters, artificial accretion occurs as sediments accumulate (+3 to +6 m/yr). However, this benefit is often counterbalanced by localized severe erosion on the downdrift side (-4 to -6 m/yr), where sediment starvation accelerates retreat. These contrasting outcomes illustrate how structural interventions may protect critical assets locally but redistribute erosion pressures elsewhere, creating new hotspots.

**Table 1:** Coastline change rates in Nakhon Si Thammarat Province (1990–2025)

Coastal Sector / Location	Observed Trend	Approx. Rate of Change (m/yr)	Notes / Characteristics
Pak Phanang Bay and adjacent downdrift coast	Severe erosion	-3 to -5	Persistent multi-decadal retreat; exacerbated by sediment reduction, subsidence, and hard-structure impacts.
Southern NST muddy/mangrove coasts (outside Pak Phanang)	Moderate to high erosion	-2 to -4	Loss of mangrove buffers; locally intensified by aquaculture conversion and storm-driven erosion.
Northern sandy beaches (NST north coast)	Low to moderate erosion	0 to -2	Less affected than southern sectors; some stretches remain relatively stable.
River mouth zones (selected estuaries)	Accretion (localized)	+2 to +5	Fluvial sediment deposition leads to prograding spits and bars; short spatial extent.
Updrift side of groynes / breakwaters	Artificial accretion	+3 to +6	Sediment trapped by coastal structures; often accompanied by downdrift erosion.

Table 1 highlight the complexity of coastline change in NST. Natural processes such as monsoon storms, sea-level rise, and sediment flux underpin the overall dynamics, yet human activities, particularly mangrove clearance, aquaculture development, and the placement of coastal structures play a decisive role in amplifying or reshaping erosion patterns. The juxtaposition of updrift accretion with downdrift retreat around engineered defenses demonstrates the inherent trade-offs of hard-engineering approaches, while the success of localized mangrove restoration projects points to the potential of nature-based solutions. These findings underscore the importance of integrated coastal zone management that moves beyond piecemeal interventions. Effective long-term strategies must combine sediment management, ecological restoration, and carefully planned protective structures to address erosion comprehensively while minimizing the creation of new vulnerabilities.

### 3.6 Drivers of Coastline Change

The spatial patterns observed are the result of multiple, interacting drivers:

- Sediment budget imbalance: River regulation and watershed land-use changes have reduced sediment delivery to the coast.
- Relative sea-level rise: Global sea-level rise combined with localized subsidence has increased inundation risk.
- Storm events: Tropical storms and northeast monsoons (September–January) produce episodic coastline retreat.
- Land-use change: Large-scale mangrove clearance for aquaculture has diminished coastline stability.
- Coastal engineering: While groynes, breakwaters, and seawalls provide protection locally, they frequently intensify erosion in adjacent areas.

### 3.7 Implications for Coastal Communities and Ecosystems

The observed erosion has profound socio-economic and ecological consequences. Productive agricultural land and fishponds are being lost in Hua Sai and Pak Phanang, while communities face heightened flooding risks. Coastal ecosystems, particularly mangroves, have declined in both extent and function, undermining biodiversity and natural coastline defenses. Tourism along northern sandy beaches has been less affected, but ongoing retreat threatens the long-term sustainability of beach-based livelihoods.

### 3.8 Future Projections

The trend of coastal erosion is expected to continue and potentially accelerate. Projections from climate change models and vulnerability assessments indicate that sea level rise will be a significant driver of future coastline retreat. A study projecting future scenarios for Nakhon Si Thammarat found that by 2100, a sea level rise of 124.38 cm could lead to a beach retreat of 507.90 m, resulting in a loss of 1.49 km<sup>2</sup> of sand. This highlights the long-term threat posed by climate change and the need for proactive adaptation strategies beyond just hard engineering solutions.

## 4. Conclusion

This research highlights both the dynamics and the methodological innovation underpinning multi-decadal coastline monitoring in Nakhon Si Thammarat. By integrating AWEI and Otsu thresholding into a GEE-based pipeline, the study delivers a fully automated and reproducible framework for extracting coastlines across diverse geomorphic settings. Unlike conventional approaches that depend on manual thresholding or site-specific adjustments, this workflow ensures consistency, scalability, and transparency, making it particularly valuable for long-term and large-area applications. The results confirm stark spatial contrasts, with severe erosion in southern muddy coasts, relative stability on northern sandy beaches, and strong accretion at Laem Talumphuk. More importantly, the methodological advance demonstrates that high-quality, multi-decadal records can be generated rapidly using freely available satellite archives and cloud computing, lowering technical and resource barriers for coastal monitoring. This innovation underscores the potential for remote-sensing workflows not only to document past changes but also to inform integrated coastal management, where nature-based solutions such as mangrove rehabilitation can be balanced with engineering interventions to enhance resilience against future sea-level rise and storm impacts.

## 5. Limitations

This study, while providing valuable insights into multi-decadal coastal dynamics in Nakhon Si Thammarat, is subject to several limitations. First, the use of Landsat imagery, with its 30-meter spatial resolution, restricted the detection of fine-scale shoreline fluctuations and subtle geomorphological changes. Smaller features such as narrow sand spits, erosion scarp lines, or localized mangrove patches may therefore have been underrepresented. Second, validation of the remotely sensed results was constrained by the limited availability of high-

resolution imagery and in-situ measurements, reducing the ability to fully verify the accuracy of coastline positions. Third, despite the combined use of AWEI and Otsu thresholding, misclassifications occasionally occurred in areas of agricultural expansion, seasonal flooding, and mangrove transition zones, where spectral characteristics overlapped between land and water. Finally, while the study identified patterns of erosion and accretion, the attribution of these changes to specific natural and anthropogenic drivers such as dam construction, subsidence, or engineered structures remained qualitative due to the absence of detailed hydrodynamic, sediment transport, and socio-economic datasets.

## 6. Recommendations

Incorporating higher-resolution satellite imagery, such as Sentinel-2 or commercial datasets, alongside UAV-based mapping, would allow for the detection of finer-scale shoreline dynamics and improve accuracy in complex coastal settings. Greater integration of field-based validation campaigns is also recommended to calibrate remote sensing outputs and reduce uncertainty in coastline extraction. In addition, coupling remote sensing with hydrodynamic and sediment transport models would enable a more quantitative assessment of the relative contributions of natural processes and human activities to erosion and accretion patterns. Expanding the scope of analysis to include socio-economic dimensions such as impacts on fisheries, agriculture, and coastal infrastructure would enhance the policy relevance of the findings. Furthermore, scenario-based modeling using sea-level rise and climate projections is needed to anticipate future shoreline changes and guide long-term adaptation strategies. Finally, emphasis should be placed on evaluating the effectiveness of nature-based solutions, such as mangrove rehabilitation, bamboo fencing, and hybrid protection systems, which may offer more sustainable alternatives to hard-engineering approaches for strengthening coastal resilience in Nakhon Si Thammarat and similar environments.

## References

- [1] Luijendijk, A., Hagenaars, G., Ranasinghe, R., Baart, F., Donchyts, G. and Aarninkhof, S., (2018). The State of the World's Beaches. *Scientific Reports*, Vol. 8(1). <https://doi.org/10.1038/s41598-018-24630-6>.
- [2] Simons, W. J. F., Naeije, M. C., Brown, B. E., Niemnil, S., Pradit, S., Thongtham, N., Mustafar, M. A., Towatana, P., Darnsawasdi, R., Yucharoen, M. and Visser, P. N. A. M., (2019). Vertical Motion of Phuket Island (1994–2018) due to the Sumatra-Andaman Mega-Thrust Earthquake Cycle: Impact on Sea-Level and Consequences for Coral Reefs. *Marine Geology*, Vol. 414, 92–102. <https://doi.org/https://doi.org/10.1016/j.margeo.2019.05.008>.
- [3] Chawalit, C., Boonpook, W., Sitthi, A., Torsri, K., Kamthonkiat, D., Tan, Y., Suwansaard, A. and Nardkulpat, A., (2025). Geoinformatics and Machine Learning for Shoreline Change Monitoring: A 35-Year Analysis of Coastal Erosion in the Upper Gulf of Thailand. *ISPRS International Journal of Geo-Information*, Vol. 14(2). <https://doi.org/10.3390/ijgi14020094>.
- [4] Saengsupavanich, C., Chonwattana, S. and Naimsampao, T., (2009). Coastal Erosion through Integrated Management: A Case of Southern Thailand. *Ocean & Coastal Management*, Vol. 52, 307–316. <https://doi.org/10.1016/j.ocecoaman.2009.03.005>.
- [5] Cheewinsiriwat, P., Langkulsen, U., Lertwattanamongkol, V., Poompongthai, W., Lambonmung, A., Chamchan, C., Boonmanunt, S., Nakhapakorn, K. and Moses, C., (2024). Assessing Coastal Vulnerability to Climate Change: A Case Study of Nakhon Si Thammarat and Krabi. *Social Sciences*, Vol. 13(3). <https://doi.org/10.3390/socsci13030142>.
- [6] Ding, Y., Yang, X., Jin, H., Wang, Z., Liu, Y., Liu, B., Zhang, J., Liu, X., Gao, K. and Meng, D., (2021). Monitoring Coastline Changes of the Malay Islands Based on Google Earth Engine and Dense Time-Series Remote Sensing Images. *Remote Sensing*, Vol. 13(19). <https://doi.org/10.3390/rs13193842>.
- [7] Kathirolu, R., Madhumitha, P. S., Achyut Prasad, D. C. and Sandhiya, S., (2025). Spatiotemporal Analysis of Mangroves Using Median Composites and Convolutional Neural Network. *Scientific Reports*, Vol. 15(1). <https://doi.org/10.1038/s41598-025-12689-x>.
- [8] Yancho, J. M. M., Jones, T. G., Gandhi, S. R., Ferster, C., Lin, A. and Glass, L., (2020). The Google Earth Engine Mangrove Mapping Methodology (GEEMMM). *Remote Sensing*, Vol. 12(22). <https://doi.org/10.3390/rs12223758>.

- [9] Pinkeaw, S., Boonrat, P., Koedsin, W. and Huete, A., (2024). Semi-Automated Mangrove Mapping at National-Scale using Sentinel-2, Sentinel-1, and SRTM Data with Google Earth Engine: A Case Study in Thailand. *The Egyptian Journal of Remote Sensing and Space Sciences*, Vol. 27(3), 555–564. <https://doi.org/10.1016/j.ejrs.2024.07.001>.
- [10] Pimple, U., Simonetti, D., Sitthi, A., Pungkul, S., Leadprathom, K., Skupek, H., Som-ard, J., Gond, V. and Towprayoon, S., (2017). Google Earth Engine Based Three Decadal Landsat Imagery Analysis for Mapping of Mangrove Forests and Its Surroundings in the Trat Province of Thailand. *Journal of Computer and Communications*, Vol. 6, 247–264. <https://doi.org/10.4236/jcc.2018.61025>.
- [11] Lin, P., Wei, X., Zhang, Y., Lv, P., Liu, M., Yang, Y. and Dong, X., (2025). Quantifying Spatiotemporal Evolution of Sandy Shorelines in Northern China Using DSAS: A Case Study from Dalian World Peace Park. *Sustainability*, Vol. 17(17). <https://doi.org/10.3390/su17177591>.
- [12] Curoy, J., Ward, R., Barlow, J., Moses, C. and Nakhapakorn, K., (2022). Coastal dynamism in Southern Thailand: An application of the CoastSat toolkit. *PLOS ONE*, Vol. 17. <https://doi.org/10.1371/journal.pone.0272977>.
- [13] Nidhinarangkoon, P., Ritphring, S., Kino, K. and Oki, T., (2023). Shoreline Changes from Erosion and Sea Level Rise with Coastal Management in Phuket, Thailand. *Journal of Marine Science and Engineering*, Vol. 11(5). <https://doi.org/10.3390/jmse11050969>.
- [14] Noonsuk, W., (2012). The Urban Development in Nakhon Si Thammarat (Peninsular Thailand). Based on Preliminary Results of Excavations. *Bulletin de l'Ecole Française d'Extrême-Orient*, Vol. 99, 331–349. <https://doi.org/10.3406/befeo.2012.6158>.
- [15] Thepsiriamnuay, H. and Pumijumngong, N., (2024). Sandy Beach Erosion: Impacts and Adaptation Strategies in Thailand. *Environment, Development and Sustainability*. <https://doi.org/10.1007/s10668-024-04763-7>.
- [16] Nimmate, P., Pailoplee, S., Choowong, M. and Visedpadsa, S., (2023). *Evidence of Coastal Landforms and Age Determination Related to the Sea- Level Change at Nakhon Si Thammarat province In Southern Thailand*. Vol. 45, 363–370.
- [17] Langkulsen, U., Cheewinsiriwat, P., Rwodzi, D. T., Lambonmung, A., Poompongthai, W., Chamchan, C., Boonmanunt, S., Nakhapakorn, K. and Moses, C., (2022). Coastal Erosion and Flood Coping Mechanisms in Southern Thailand: A Qualitative Study. *International Journal of Environmental Research and Public Health*, Vol. 19(19). <https://doi.org/10.3390/ijerph191912326>.
- [18] Ratri, D., Mizuno, K. and Martono, D., (2021). The Effectiveness of Breakwaters Decreasing the Peat Shoreline Change in Bengkalis Island. *IOP Conference Series: Earth and Environmental Science*, Vol. 802. <https://doi.org/10.1088/1755-1315/802/1/012007>.
- [19] Thammaboribal, P., Tripathi, N. K., Lipiloet, S. and Mandadi, R., (2025). Flood Mapping and Damage Assessment Using UN-SPIDER Recommended Practices in Google Earth Engine: A Case Study of the 2024 Chiang Rai Flood, Thailand. *International Journal of Geoinformatics*, Vol. 21(3), 165–179. <https://doi.org/10.52939/ijg.v21i3.4039>.
- [20] Arunplod, C., Phonphan, W., Wongsongja, N., Utarasakul, T., Niemmanee, T., Daraneesrisuk, J. and Thongdara, R., (2023). Spatial Dynamics Evolution of Land use for the Study of the Local Traditional Living Changes. *International Journal of Geoinformatics*, Vol. 19(4), 37–49. <https://doi.org/10.52939/ijg.v19i4.2635>.
- [21] Feyisa, G. L., Meilby, H., Fensholt, R. and Proud, S. R., (2014). Automated Water Extraction Index: A New Technique for Surface Water Mapping Using Landsat imagery. *Remote Sensing of Environment*, Vol. 140, 23–35. <https://doi.org/10.1016/j.rse.2013.08.029>.
- [22] Yan, P., Fang, Y., Chen, J., Wang, G. and Tang, Q., (2023). Automated Extraction for Water Bodies Using New Water Index from Landsat 8 OLI Images. *Journal of Geodesy and Geoinformation Science*, Vol. 6(1), 59–75. <https://doi.org/10.11947/j.JGGS.2023.0105>.
- [23] Liu, S., Wu, Y., Zhang, G., Lin, N. and Liu, Z., (2023). Comparing Water Indices for Landsat Data for Automated Surface Water Body Extraction under Complex Ground Background: A Case Study in Jilin Province. *Remote Sensing*, Vol. 15(6). <https://doi.org/10.3390/rs15061678>.
- [24] Ciecholewski, M., (2024). Review of Segmentation Methods for Coastline Detection in SAR Images. *Archives of Computational Methods in Engineering*, Vol. 31(2), 839–869. <https://doi.org/10.1007/s11831-023-10000-7>.

- [25] Zheng, J., Gao, Y., Zhang, H., Lei, Y. and Zhang, J., (2022). OTSU Multi-Threshold Image Segmentation Based on Improved Particle Swarm Algorithm. *Applied Sciences*, Vol. 12(22). <https://doi.org/10.3390/app122211514>.
- [26] Tang, W., Zhao, C., Lin, J., Jiao, C., Zheng, G., Zhu, J., Pan, X. and Han, X., (2022). Improved Spectral Water Index Combined with Otsu Algorithm to Extract Muddy Coastline Data. *Water*, Vol. 14(6). <https://doi.org/10.3390/w14060855>.
- [27] Khomsin, K., Nusantara, C. A. D. S. and Saputra, B., (2024). Integration of AWEI and Otsu Threshold Algorithms for Maritime Boundary Delimitation: A Case Study of the Russia-Ukraine Conflict in the Sea of Azov. *BIO Web of Conferences*, Vol. 89. <https://doi.org/10.1051/bioconf/20248907005>.
- [28] Donchyts, G., Schellekens, J., Winsemius, H., Eisemann, E. and de Giesen, N., (2016). A 30 m Resolution Surface Water Mask Including Estimation of Positional and Thematic Differences Using Landsat 8, SRTM and OpenStreetMap: A Case Study in the Murray-Darling Basin, Australia. *Remote Sensing*, Vol. 8(5). <https://doi.org/10.3390/rs8050386>.
- [29] Sengupta, D., Choi, R., Tian, B., Brown, S., Meadows, M., Hackney, C. R., Banerjee, A., Li, Y., Chen, R. and Zhou, Y., (2023). Mapping 21st Century Global Coastal Land Reclamation. *Earth's Future*, Vol. 11(2). <https://doi.org/10.1029/2022EF002927>.
- [30] Chang, K., Yue, W., Wang, H., Tan, K., Liu, X., Cao, X. and Chen, W., (2025). Research on the Method of Extracting Water Body Information in Central Asia Based on Google Earth Engine. *Water*, Vol. 17(6). <https://doi.org/10.3390/w17060804>.
- [31] Sergi, G., Bocchino, F., Ravanelli, R. and Crespi, M., (2025). Monitoring Water Reservoirs Extent with Segment Anything Model applied to Sentinel imagery. *European Journal of Remote Sensing*, Vol. 58(1). <https://doi.org/10.1080/22797254.2025.2527248>.
- [32] Yulianto, F., Kushardono, D., Budhiman, S., Nugroho, G., Chulafak, G., Dewi, E. and Pambudi, A., (2022). Evaluation of the Threshold for an Improved Surface Water Extraction Index Using Optical Remote Sensing Data. *The Scientific World Journal*, Vol. 2022. <https://doi.org/10.1155/2022/4894929>.
- [33] Department of Marine and Coastal Resources. (2019). *Marine and Coastal Resources Information Nakhon Si Thammarat Province*. Ministry of Natural Resources and Environment.
- [34] Department of Marine and Coastal Resources. (2023). *Situation Report Marine and Coastal Resources and Coastal Erosion Nakhon Si Thammarat Province*. Ministry of Natural Resources and Environment.
- [35] Pungpa, S. and Chumkiew, S., (2025). Increasing Area of Banlaem Mangrove Forest at Nakhon Si Thammarat in Southern Thailand: Land Cover Changes and Predictive Models. *Journal of Environmental & Earth Sciences*, Vol. 7, 453–468. <https://doi.org/10.30564/jees.v7i5.8264>.
- [36] Thepsiriamnuay, H. and Pumijumnong, N., (2019). Climate Change Impact on Sandy Beach Erosion in Thailand. *Chiang Mai Journal of Science*, Vol. 46(5), 960–974.
- [37] Thampanya, U., Vermaat, J., Sinsakul, S. and Panapitukkul, N., (2006). Coastal Erosion and Mangrove Progradation of Southern Thailand. *Estuarine, Coastal and Shelf Science*, Vol. 68, 75–85. <https://doi.org/10.1016/j.ecss.2006.01.011>.
- [38] Aminti, P. and Billi, P., (1984). An Investigation of the Effects of Breakwaters on Beach Sediment Characteristics. *CATENA*, Vol. 11(1), 391–400. [https://doi.org/10.1016/S0341-8162\(84\)80034-X](https://doi.org/10.1016/S0341-8162(84)80034-X).
- [39] Sunkur, R., Kantamaneni, K., Bokhoree, C. and Ravan, S., (2023). Mangroves' Role in Supporting Ecosystem-Based Techniques to Reduce Disaster Risk and Adapt to Climate Change: A review. *Journal of Sea Research*, Vol. 196. <https://doi.org/10.1016/j.seares.2023.102449>.